

Hierarchical approach to energy system modelling: Complexity reduction with minor changes in results



Dmitrii Bogdanov*, Ayobami Solomon Oyewo, Christian Breyer

LUT University, Yliopistonkatu 34, 53850, Lappeenranta, Finland

ARTICLE INFO

Handling Editor: Neven Duic

Keywords:

Energy system modelling
Renewable energy
Optimisation
Defossilisation

ABSTRACT

The energy transition plays a crucial role in the ongoing process of defossilisation and carbon emissions reduction. Considering the substantial cost of the transition and importance of the energy system for the global economy, the transition must be accurately modelled to allow future system development analyses and discussions to avoid stranded investments and guarantee a reliable energy supply at every transition step. Energy system models must be operated with a technology-rich portfolio in high temporal and spatial resolution to properly estimate the impact of renewable energy variability and the role of storage and sector coupling technologies. Consequently, modern energy system models comprise tens of millions of variables and constraints, and demand vast computational resources for optimisation. This study proposes a hierarchical approach to run simulations based on partial regional disaggregation as a solution to decrease computational time without significant change in the modelling results. The discussed method is tested on the case of Japan and shows that the hierarchical approach allows for a reduction in computational time by a factor of 2.3–3.3 compared to the full spatial resolution simulation approach, while the installed capacities and costs of the energy system stay within a ±3% range for all steps of the transition through 2020 to 2050.

1. Introduction

Evidence of the ongoing climate change process is strong and is hard to disregard [1]. Together with improved understanding of the long-term effect on civilisation and the role of anthropogenic greenhouse gas (GHG) emissions in the climate change process, the international community, individual countries, cities, societies and stakeholders have been pushed to foster GHG emissions reduction efforts across all human activities, in particular in the energy system, which contributes the highest share [1]. The global community has pledged GHG emissions targets to keep the global warming effect at the level of 1.5 °C, as aimed for in the Paris Agreement. This target will ultimately demand a rapid reduction of GHG emissions in the coming decades and full carbon neutrality by 2050, or even negative CO₂ emissions in the 2040s and beyond. Most importantly, the target demands fast and sharp changes in the energy system, as it is responsible for about 80% of global GHG emissions [2]. Thus, the energy transition will play a vital role in the defossilisation of energy and the economy in general on the way to full carbon neutrality. The transition towards renewable energy (RE) does not simply fit the emission reduction narrative, it also leads to a

low-cost energy supply and lower reliance on energy imports, as the access to low-cost RE sources [3,4], the ongoing progress in energy storage technology, modern electrified mobility, and industrial processes are new drivers for the energy transition. Energy system electrification will lead to comprehensively integrated and coupled energy sectors [5,6] with new emerging technologies such as CDR [7] and desalination [8] and, consequently, to significant growth of the overall system efficiency and further energy cost decline [8,9].

The energy transition towards higher shares of renewables in the energy supply, higher electrification, and comprehensive energy sector integration is a sophisticated process that demands significant time and investments. That makes the proper long-term planning extremely important to choose an optimal transition pathway that avoids stranded investments and reaches the climate targets in time. Many energy system models have been developed in recent years to support decision making [10,11]. The main trend in energy system modelling development is the growing complexity of the applied models following important requirements. First, a high temporal resolution is required to properly consider the effects of the variable RE (VRE) sources and estimate demand in storage capacity and other flexibility options, and hourly

* Corresponding author.

E-mail address: dmitrii.bogdanov@lut.fi (D. Bogdanov).

resolution has been found to allow adequate simulation of the operation of VRE based systems [12]. For fossil-based systems and systems with high shares of fossil fuels, less advanced annual balancing models in hourly resolution can still be used [10,13]. Second, a multi-nodal approach to enable a sufficiently high spatial resolution must be considered to avoid any copper plate effect [14,15], which leads to averaging of RE generation profiles and leads to an underestimation of RE generation variability [16,17] and grid interconnection costs [5]. System integration simulation requires technology-rich portfolios of models, the broad application of sector coupling technologies, and simulation of all energy system sectors in one run. That can be seen in the energy system models portfolio, as shown by Lopez et al. [18]. Most of the active models use full hourly resolution (EnergyPLAN [19,20], the LUT Energy System Transition Model (LUT-ESTM) [8,21–23], HOMER [24], REMix [25], AU model [15], PyPSA [26], LOADMATCH [27], NEMO [28], ISA model [29], H2RES [30]) or at least a time-slices approach (TIMES [31], GENeSYS-MOD [32]). More than half of the models introduced a multi-nodal approach to simulation. Also, models are developed to introduce more energy sectors rather than study only the power sector and model the individual sectors in higher detail, for example, tracing non-energetic demand of fuels and chemicals in various industries, and CO₂ emissions from limestone processing in the latest versions of LUT-ESTM [23], PyPSA [33], or versions of TIMES [34]. Furthermore, the transition pathway optimisation demands energy system optimisation for each step of the transition, for the case of a myopic approach, or all the transition at once, for the case of a perfect foresight approach. Independent of the approach, the transition optimisation leads to longer modelling time.

Such model development and expansion and continued improvements of all these aspects lead to the continuous growth of the model size. In the LUT-ESTM tool, the number of variables is already in the order of millions for single node and tens of millions for multi-node simulations, and that consequently increases the demand for computational capacities and the time for optimisation. Despite the growing computational capacities, novel approaches in energy system modelling are needed to decrease energy systems simulation complexity without loss of the RE technologies simulation reliability and allow further growth in detailing of energy system models, in particular broader technology portfolios, higher regional, and temporal resolution. New methods to enable such high resolution for more detailed studies without increase in model complexity, or to reduce modelling time, represent the major research gap in the field of energy system transition research.

Preferably such methods should be applicable to any existing model, as these concentrate on the better refining of the inputs in general rather than the model itself. Currently, most efforts are concentrated on the assessment of the impact of different time-series aggregations methods as discussed in Kotzur et al. [35] and the development of novel methods of temporal aggregation to increase the reliability of the time-series approach as researched in Hoffmann et al. [36]. Teichgraeber and Brandt [37] provide an overview of existing time-series aggregation methods. Other studies propose advanced methods of an optimal regional structure definition and spatial resolution reduction as described in Frysztacki et al. [38] to decrease models' complexity. The computational time reduction can reach a factor of up to 50 for the times-series case [35], or even higher [37]. The impact of spatial resolution reduction claimed to be significant while the value depends on the applied resolution [38,39] and it can be seen that higher spatial resolution leads to better results. However, spatial resolution reduction naturally leads to significant deviations in the results of energy system optimisation with high shares of renewables [39]. Similarly, different methods of temporal aggregation lead to sensitive changes in the system optimisation results as can be seen in numerous studies [35,40]. For temporal aggregation Teichgraeber and Brandt [37] highlight different sources of errors, while the proper choice of the period represents the main challenge of time-series aggregation, proper linking and

interaction of different time-series within the model has to be reached to allow credible results. The target is to find methods that allow a complexity reduction without change in simulation results and without modifications of the main model.

This article presents a novel method to reduce the energy system transition modelling complexity without reduction of the results reliability. This study introduces a novel hierarchical approach in multi-regional studies which is supposed to be applicable to any model with multi-nodal capabilities, thus filling this research gap. This novelty allows substituting the simulation of an integrated multi-regional energy system by a simulation in a reduced regional resolution (macro-region level) followed by simulations in full regional and hourly resolution for each of the macro-regions in order to combine the reduced computational time of lower spatial resolution and the improved quality of results in high resolution. Despite the increased number of optimisation runs, the models on each level contain a smaller number of variables and are optimised faster, leading to reduced integrated simulation time for a given energy system. To the authors' knowledge, such a method has not yet been discussed and examined for integrated energy system modelling. The main motivation behind this novel approach is to significantly reduce the model size at each simulation step and the overall simulation time without notable change in the transition pathway or structure of the modelled energy system, in order to allow energy system transition studies in higher regional resolution.

2. Methods and data

The proposed method is applied to the LUT-ESTM [8,22,23], which is designed to simulate energy transitions for integrated power, heat, transport, and industry sectors. For each time step, the model defines an optimal structure of an integrated energy system and operation modes of each system element to reach a least cost optimum of the entire energy system under given financial and technical assumptions as well as region or scenario specific conditions, which consider societal choices. The LUT-ESTM performs linear optimisation for the full energy system, or specific sectors, in an hourly resolution for each step of the transition, which increases the reliability of the results in comparison to annual energy demand balancing or time series-based approaches. For the given study, the LUT-ESTM used the Mosek optimiser (version 7) [41]. The LUT-ESTM allows for energy system simulation in high spatial resolution with individual regional energy systems interconnected with high voltage alternating current (HVAC) and high voltage direct current (HVDC) grids. The target of the optimisation is the minimisation of the total integrated energy system cost. The model describes the transition of power, heat, transport, and industry sectors and covers all energy demand and most anthropogenic GHG emissions. The model defines the optimal structure and operation of the integrated energy system to satisfy the given hourly demand of electricity, space heat, and domestic hot water demand, energy demand of the transport sector, and industrial demand (cement, steel, chemicals, aluminium, pulp and paper, desalination, and other industries) at each step of the transition. This optimisation also considers the energy demand, available resources, and active capacities installed in previous steps. Costs of the system are calculated as the sum of the annualised capital and operational expenditures, including ramping costs, fuel costs, and CO₂ emissions pricing for all considered technologies. Energy system transitions are typically performed for the year 2020–2050 with 5-year time steps. At each step of the transition modelling, the existing active capacity for each technology defines the lower limit for the respective technology capacity. The active capacity existing in the system is defined at each time step for each region based on the data of the capacity installed at previous steps and the lifetime for a given technology at given commissioning years as presented in Eq. (1).

$$\forall t \in [tech] \text{ } existingCap_{t,year} = \sum_{y=1960}^{year} newCap_{t,y} \bullet ((y + N_{t,y}) > year) \quad (1)$$

wherein: y , $year$ - years, t , $tech$ - generation and storage technologies, $existingCap_{t,year}$ - existing active capacity for technology t at modelled year, $newCap_{t,y}$ - new built capacity for technology t at previous year y , $N_{t,y}$ - lifetime of the capacity of technology t built in year y .

Then, the model optimisation determines the optimal regional capacity of the technologies in the given year, which defines the newly built capacity needed by the system as defined in Eq. (2).

$$\forall t \in [tech] \text{ } newCap_{t,year} = instCap_{t,year} - existingCap_{t,year} \quad (2)$$

wherein: $year$ - modelling year, t , $tech$ - generation and storage technologies, $newCap_{t,year}$ - new built capacity for technology t at given year, $instCap_{t,year}$ - total capacity for technology t at given year as defined by the model optimisation, $existingCap_{t,year}$ - existing active capacity for

technology t in region r and year y , $OPEXfix_{r,t,y}$ - fixed operational expenditures for technology t in region r and year y , $OPEXvar_{r,t,y}$ - variable operational expenditures technology t in region r and year y , $newCap_{r,t,y}$ - new built capacity for technology t built in region r at year y , $N_{t,y}$ - lifetime of the capacity of technology t built at year y , $E_{genSplit,r,t,y}$ - annual generation by technology t in region r in year by capacity built at year y , $rampCost_t$ - cost of ramping of technology t , $totRamp_{r,t}$ - sum of power ramping values during the year for the technology t in the region r .

This historical cost calculation approach considering the legacy system is also used for other cost calculations including levelised cost of electricity (LCOE) and split of LCOE in sub-categories.

The model optimiser's target function represents the minimisation of the annualised cost of the system (see Eq. (5)). The existing capacities represent the lower limit for the respective technologies capacity, thus the technologies capex on previous steps of transition has no impact on the system optimisation at the given step:

$$\min \left(\sum_{r=1}^{reg} \sum_{t=1}^{tech} \left(CAPEX_{r,t,year} \bullet crf_{r,t,year} + OPEXfix_{r,t,year} \right) \bullet instCap_{t,year} + OPEXvar_{r,t,year} \bullet E_{gen,r,t,year} + rampCost_t \bullet totRamp_{r,t} \right. \\ \left. + \sum_{l=1}^{lines} \sum_{tt=1}^{transm} \left(CAPEX_{l,tt,year} \bullet crf_{l,tt,year} + OPEXfix_{l,tt,year} \right) \bullet instCap_{tt,year} \bullet length_l \right) \quad (5)$$

technology t at modelled year.

While the target function for the optimisation only considers the financial assumptions for the given year, the energy costs calculations in the post-processing phase consider the legacy of the capacity installations and the financial assumptions in the periods when these capacities were built. For the variable operational expenditures (opex) calculations, the energy output of technologies is split accordingly to the capacity age structure as defined in Eq. (3).

wherein: $year$ - modelling year, t , $tech$ - electricity and heat generation, storage, power-to-X, tt , $transm$ - electricity transmission technologies, $CAPEX_{r,t,year}$ - capital expenditures for technology t in region r and year, $crf_{r,t,year}$ - capital recovery factor for technology t in region r and year y , $OPEXfix_{r,t,year}$ - fixed operational expenditures for technology t in region r and year y , $OPEXvar_{r,t,year}$ - variable operational expenditures technology t in region r and year y , $instCap_{t,year}$ - total capacity for technology t at given year as defined by the model optimisation, $E_{gen,r,t,year}$ - annual

$$\forall t \in [tech], \forall y \in [1960 \dots year] \text{ } E_{genSplit,t,y} = E_{gen,t,year} \bullet (newCap_{t,y} \bullet ((y + N_{t,y}) > year)) / instCap_{t,year} \quad (3)$$

wherein: $year$ - modelling year, y - all years from 1960, t , $tech$ - generation and storage technologies, $E_{genSplit,t,y}$ - annual generation by technology t by capacity built at year y , $newCap_{t,y}$ - new built capacity for technology t built at year y , $E_{gen,t,year}$ - annual generation by technology t defined by the model for the modelling year, $instCap_{t,year}$ - total capacity for technology t at given year as defined by the model optimisation, $N_{t,y}$ - lifetime of the capacity of technology t built at year y .

The annualised cost of the system at the given year is calculated accordingly to Eq. (4).

generation by technology t in region r in year, $rampCost_t$ - cost of ramping of technology t , $totRamp_{r,t}$ - sum of power ramping values during the year for the technology t in the region r , $length_l$ - length of line l in between regions.

The capacities must be sufficient to satisfy the energy (electrify, heat, e-fuels and chemicals), transport services and industrial products demand for every hour of the year as defined in balance equations for electricity, heat and other energy carriers for each hour of the year.

Transmission grids between regions play especially important role in simulation of the energy systems with high shares of RE, allowing to

$$annualCostHist_{year} = \sum_{r=1}^{reg} \sum_{t=1}^{tech} \sum_{y=1960}^{year} \left(CAPEX_{r,t,y} \bullet crf_{r,t,y} + OPEXfix_{r,t,y} \right) \bullet ((newCap_{r,t,y} \bullet ((y + N_{t,y}) > year)) + OPEXvar_{r,t,y} \bullet E_{genSplit,r,t,y} + rampCost_t \bullet totRamp_{r,t} \bullet length_l) \quad (4)$$

wherein: $year$ - modelling year, y - all years from 1960, t , $tech$ - generation and storage technologies, $CAPEX_{r,t,y}$ - capital expenditures for technology t in region r and year y , $crf_{r,t,y}$ - capital recovery factor for

access the best energy resources over the country. The transmission grids between the regions and related costs are fully covered in the model: the model defines the optimal capacity of HVAC and HVDC

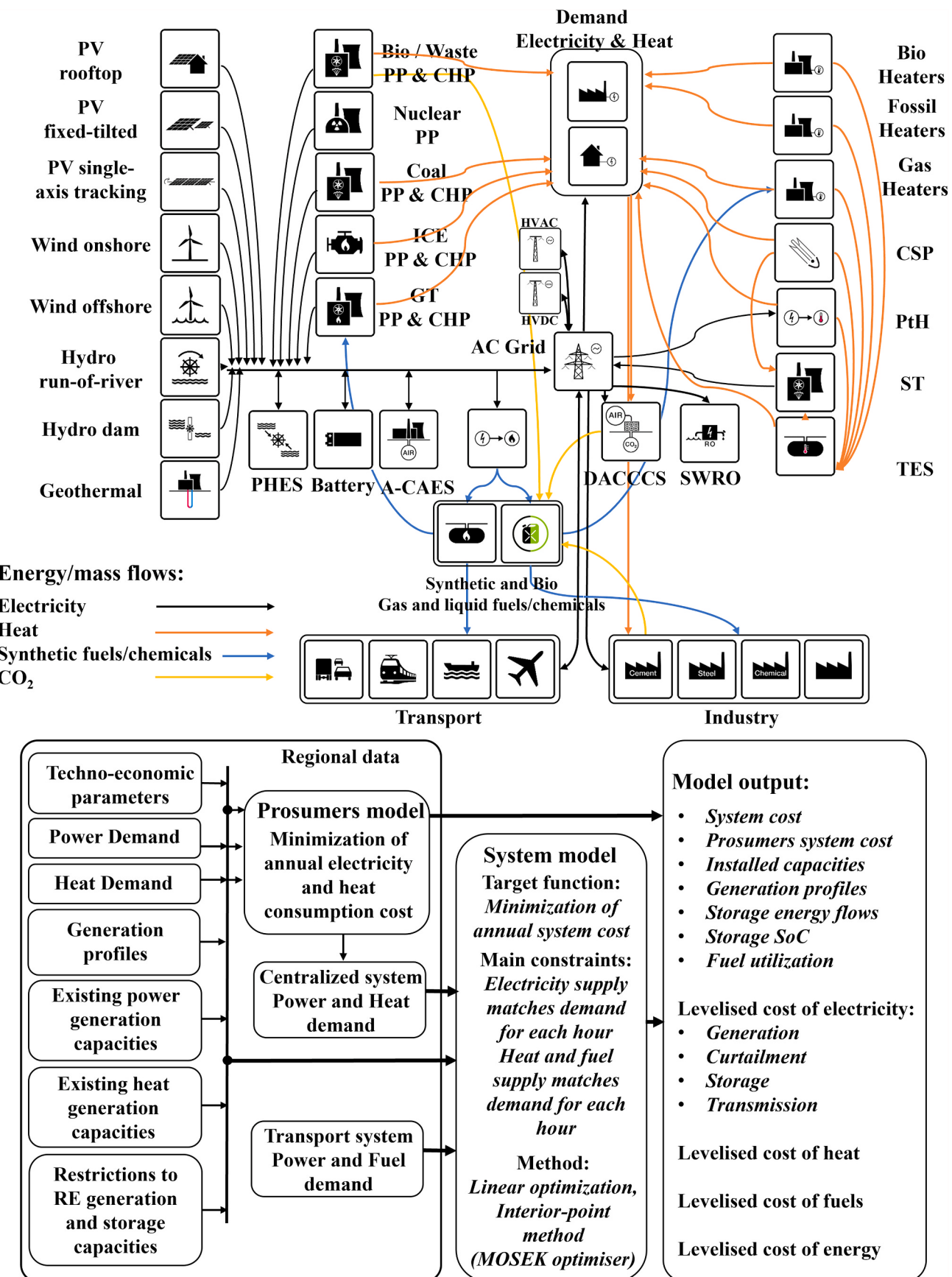


Fig. 1. Integrated energy system structure scheme and the model flowchart.

power lines considering the length of the lines, the capacity of the AC/DC converter pairs for HVDC lines, the losses in the power lines and converters. Distribution grid costs within the region are not included in the target function of the model, though the distribution losses are considered in the demand estimation.

More details on LUT-ESTM are provided in the supplementary material and the modelling approach is described in full in previous publications [22,23]. The model is based on the previous version presented in Bogdanov et al. [23]. The main modifications are the introduction of smart charging and vehicle-to-grid (V2G) function for battery-electric vehicles (BEV) and plug-in hybrid vehicles (PHEV). Additionally, the model considers the possibility of international e-fuels trading in terms of e-fuels imports. The simplified scheme of the integrated system in the LUT Energy System Transition Model is shown in Fig. 1.

2.1. Hierarchical approach to the energy system modelling

Modelling the entire energy system in hourly resolution with a technology-rich portfolio can be demanding, especially in multi-node simulations. The regional structure for a transition study with high shares of RE should be defined accurately to consider possible regional climate differences and in the right spatial resolution to avoid underestimating grid costs, averaging RE generation profiles, and thus underestimating the storage and flexible generation capacities. The regional structure should also match the regional division of the country to allow utilisation of the existing statistical data for inputs collection and facilitate the results analysis and comparison with actual data. At the same time, the number of sub-regions should not exceed a certain number to guarantee successful model simulation in an adequate amount of computation time.

2.1.1. Hierarchical simulation sequence

The proposed method combines simulations in lower and higher spatial resolution in order to integrate the reduced simulation time typical for the modelling in lower spatial resolution and high quality of results which can be acquired considering higher spatial resolution. The proposed hierarchical simulation sequence for the energy system modelling comprises four steps.

1. The first step (full resolution definition) is the definition of the optimal spatial resolution and respective data preparation. The application on the case of Japan leads to statistical data collection at the prefecture level and partially for the nine electric power companies (EPCOs) operating in mainland Japan, excluding the isolated Okinawa EPCO. Integrated energy system modelling in hourly resolution and a technology-rich portfolio would not be possible for the 47 prefectures level, so the input data was structured for the nine EPCO areas that normally follow prefectures border; only Shizuoka is divided between Tokyo and Chubu EPCOs. Finally, the territory of mainland Japan is represented in 9 sub-regions: Hokkaido, Tohoku, Tokyo, Hokuriku, Chubu, Kansai, Chugoku, Shikoku, and Kyushu as described in Eq. (6).

$$R_1 \cup R_2 \cup R_3 \cup R_4 \cup R_5 \cup R_6 \cup R_7 \cup R_8 \cup R_9 \in J \quad (6)$$

wherein: $R_1, R_2 \dots R_9$ represent individual EPCO areas and J – the whole mainland Japan.

2. In the second step (aggregation to macro-regions and simulation), the spatial resolution is decreased to reduce the number of regions and the respective model complexity. The definition of these macro-regions must be aligned with the local conditions for balance of the regions and comparable resource conditions of the aggregated sub-regions. For the case of Japan, this leads to three macro-regions: Three northeast sub-regions (Hokkaido, Tohoku, and Tokyo EPCOs areas) were aggregated into one Northeast region, as the grid

frequency in these sub-regions differs from the rest of the country, and all these sub-regions possess better than average wind resources. Three central sub-regions (Hokuriku, Chubu, and Kansai) are aggregated into the Centre macro-region. Kyushu, Chugoku, and Shikoku sub-regions are aggregated into the Southwest macro-region. Then, the energy system transition is modelled for the reduced regional structure consisting of only 3 macro-regions, as described in Eq. (7). The results of this simulation represent the pathway of the transition, and, for each time step of the transition, the results define the optimal energy system structure and power flows between the macro-regions as described in Eq. (8). Though the results of the simulation in the reduced spatial resolution suffer due to an underestimated variability of the RE resources and do not present detailed information on the RE installation distribution inside the macro-regions, the data on the power flows among the macro-regions provides insights on the energy exchange inside the country.

$$McR_1 \cup McR_2 \cup McR_3 \in J \quad (7)$$

$$ELgen_{mc,h} - ELdem_{mc,h} - ELcurt_{mc,h} = \sum_{mcn} Elexp_{mc,mcn,h} \\ \bullet (1 - gl_{mc,mcn}) - ELimp_{mc,mcn,h} \bullet (1 - gl_{mc,mcn}) \quad (8)$$

wherein: McR_1, McR_2, McR_3 represent macro-regions and J – the whole mainland Japan. mc – macro-region, mcn – neighbouring macro-region, h - hour of the year, $ELgen$ – electricity generation, $ELdem$ – electricity demand, $ELcurt$ – electricity curtailment (excess), $Elexp$ – electricity exports, $ELimp$ – electricity imports, gl – grid losses.

3. In the third step (separate macro-regions solutions) of the simulation sequence, each of the macro-regions is modelled in full regional resolution (Eqs. (9)–(11)). Each macro-region is modelled individually as an energy island, the power flows from the results of the simulation in reduced spatial resolution (second step) are added to the power balancing equations of the bordering sub-regions (Eq. (12)) to consider electricity exchange between macro-regions. If the macro-regions are interconnected via several sub-regions (i.e. Northeast and Central macro-regions are connected by the Tokyo-Chubu and Tohoku-Hokuriku lines), the energy flows from results of the second step are divided among these sub-regions accordingly to existing grid interconnection capacity, or equally if existing capacity is not sufficient and new grids have to be built. Finally, the energy flows between macro-regions are considered in the additional flows added to the sub-region's electricity balance constraint as shown in Eq. (13).

$$R_1 \cup R_2 \cup R_3 \in McR_1 \quad (9)$$

$$R_4 \cup R_5 \cup R_6 \in McR_2 \quad (10)$$

$$R_7 \cup R_8 \cup R_9 \in McR_3 \quad (11)$$

$$ELgen_{r,h} - ELdem_{r,h} - ELcurt_{r,h} + ELadd_{r,h} \\ = \sum_m Elexp_{rn,t} \bullet gl_{rn,t} - ELimp_{rn,t} \bullet gl_{rn,t} \forall r, rn \in McR \quad (12)$$

$$\sum_r ELadd_{r,h} = \sum_{mcn} Elexp_{mcn,t} \bullet gl_{mc,mcn,t} - ELimp_{mcn,t} \bullet gl_{mc,mcn,t} \quad (13)$$

wherein: $R_1, R_2 \dots R_9$ represent individual EPCO areas, McR_1, McR_2, McR_3 represent macro-regions. r – sub-region, rn – neighbouring sub-region, McR – macro-region to which these region and neighbouring regions belong to, h - hour of the year, $ELgen$ – electricity generation, $ELdem$ – electricity demand, $ELcurt$ – electricity curtailment (excess), $ELadd$ – additional electricity flows representing the electricity flows

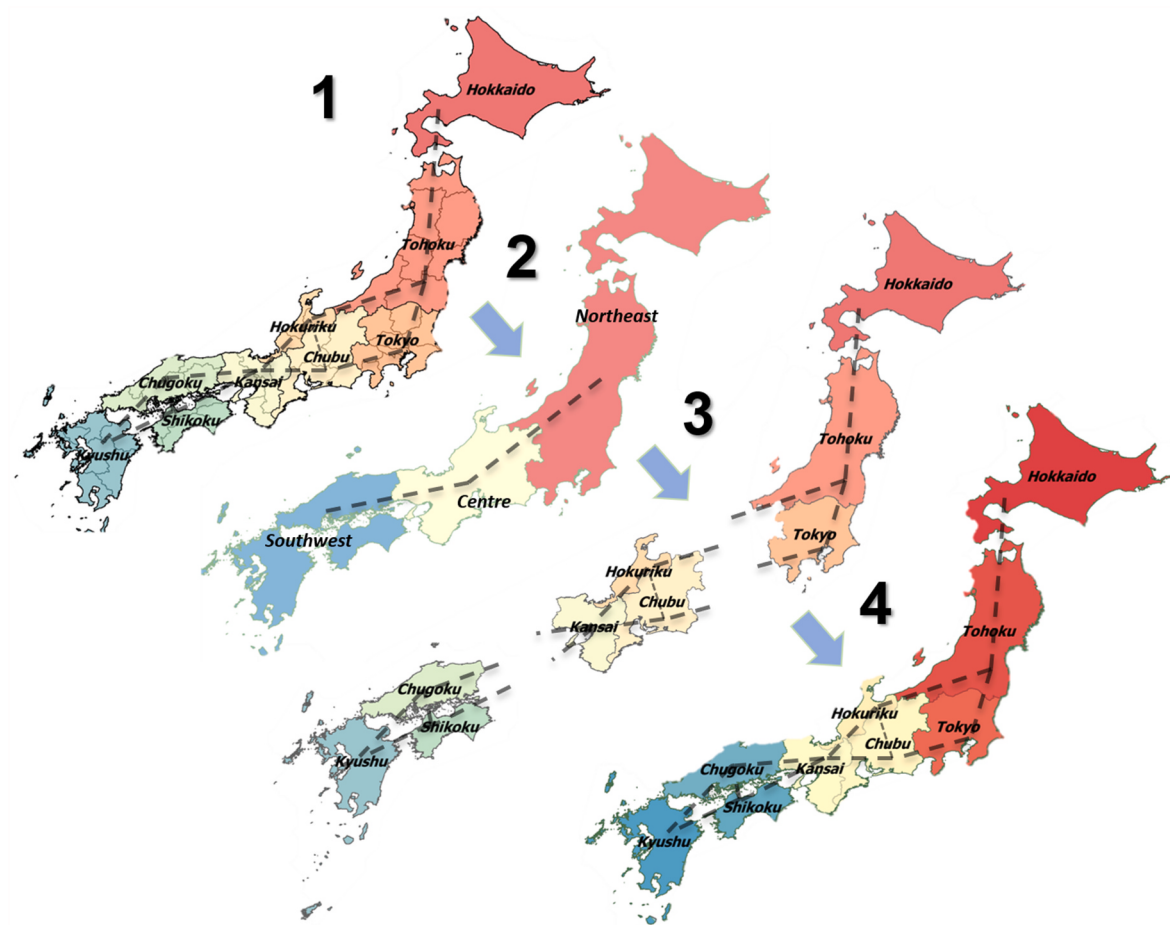


Fig. 2. Schematic representation of the hierarchical simulation sequence for the case of Japan.

between macro-regions, $ELexp$ – electricity exports, $ELimp$ – electricity imports, gl – grid efficiency, mc – macro-region to which region r – belongs to, mcn – neighbouring macro-region.

- In the fourth step (full resolution results), the results of each macro-region simulation in higher spatial resolution are tied back to represent the results of the fully integrated energy system of a country or region (see Eq. (14)). For the case of Japan, the results of all three macro-region simulations are merged, and regional energy system structures, operational results, grid structures, and operation inside macro-regions are directly taken from the results. The power flows between sub-regions at the macro-regions borders and respective grid capacities are calculated based on the simulation results in reduced spatial resolution (second step). Merged results fully reproduce the format of the results of the simulation in full regional resolution. The electricity flows for the reconstructed results in 9 sub-regions resolution are presented in Eq. (15).

$$R_1 \cup R_2 \cup R_3 \cup R_4 \cup R_5 \cup R_6 \cup R_7 \cup R_8 \cup R_9 \in J \quad (14)$$

$$ELgen_{r,h} - ELdem_{r,h} - ELcurt_{r,h} = \sum_{m \in mcn} ELexp_{m,t} \bullet gl_{r,m,t} - ELimp_{m,t} \\ \bullet gl_{r,m,t} \forall r \subset J \quad (15)$$

wherein: $R_1, R_2 \dots R_9$ represent individual EPCO areas and J – the whole mainland Japan, r – sub-region, m – neighbouring sub-region, h - hour of the year, $ELgen$ – electricity generation, $ELdem$ – electricity demand, $ELcurt$ – electricity curtailment (excess), $ELexp$ – electricity exports, $ELimp$ – electricity imports, gl – grid efficiency.

A schematic representation of the hierarchical simulation sequence applied on the case of Japan is presented in Fig. 2.

This approach can be used for simulation in even higher resolution, as the third step could be repeated to further increase the resolution and simulate each region in prefectures resolution for the case of Japan. Such a level of detail was not performed in this study as a level of nine sub-regions was considered sufficient, and verification via a classic simulation in 47 prefectures resolution could not be performed due to too high complexity. The level of detail could be further increased by embedding Japan in an energy system transition for the whole Northeast Asia region [21,42], which would also enable modelling of coupled energy systems for the entire major region. In general, the hierarchical approach allows to model an energy system in high geographic detail as a sequence of two or more steps so that a highly complex simulation problem can be separated into a multi-level simulation task, for instance in a five level approach on the case of Japan: Northeast Asia as a global major region (first level), Japan as a country in Northeast Asia (second level), the three macro-regions of Japan (third level), then nine sub-regions of Japan (fourth level), the 47 prefectures of Japan (fifth level). That principle can be applied to all regions in the world and independently of the used energy system model and that would allow to model the world in thousands of regions [7].

2.1.2. Variable renewable energy profiles for hierarchical simulations

The RE profiles for individual sub-regions are calculated based on weather data for the year 2005 taken from NASA [43,44] and reproduced to a higher resolution by the German Aerospace Centre [45]. The regional profiles calculation routine is described in Ref. [21]. In this routine, the locations with higher full load hour (FLh) values are given higher weights in the regional profiles calculations to reflect the reality that RE projects are developed first in locations with attractive resource

conditions.

Applied to macro-regions, this routine can lead to an increased inaccuracy in the RE profiles estimation. The RE potential can be both overestimated if the overall macro-region profile is strongly influenced by the RE conditions in the best locations, even if these locations are distant from the main demand centres, or underestimated, if the better than average locations are concentrated in part of one of the sub-regions and these locations' potential is averaged with the potential of locations in other sub-regions. Consequently, in the first case, the real cost of RE generation would be underestimated by neglecting additional transmission grid costs, and in the second case, the average FLh value in the macro-region would be too low, making the RE generation less economically attractive. In any case, the hourly capacity factor profiles averaged over bigger areas will be smoothed and lead to an underestimation of short-term storage in the system.

The impact of the RE resource aggregation effect can be reduced if the RE profiles for macro-regions are calculated as the average or weighted average of sub-regional RE profiles. The same challenge is still present on the sub-regional level because distribution grid costs are not considered, though the order of a potential error may be reduced. In the case of the weighted average approach, the weights of the individual sub-regions in the total average profile for the macro-region are estimated based on the regional energy system parameters, such as annual power demand, peak load, the average length of grid connection to neighbouring sub-regions' demand centres, RE technologies LCOE in each of the sub-regions, and average LCOE value for the whole macro-region (as if all sub-regions were weighted evenly). Formulas for the weights are presented in the supplementary material ('Macro-regions data preparation'). Though such a simplified approach obviously cannot estimate the real distribution of the RE capacities inside macro-regions, it is able to capture the main aspects of the distribution: more capacity will be installed in the region with much better RE resources than other sub-regions and it will be located closer to main demand centres. Conversely, in the case of evenly distributed resources and long distances between regional demand centres, the capacity will be distributed more evenly. For the proposed regional structure of Japan, the average and weighted average approaches resulted in very similar numbers, and, considering that the weights formula that was used is the result of approximation of global numbers, the simple average formula with equal weights was applied. Table 1 presents the results of the RE profiles calculations for three main cases.

1. RE profiles calculated for 9 sub-regions as described in Ref. [21].
2. RE profiles calculated for 3 macro-region as described in Ref. [21].
3. RE profile for macro-region calculation as an average of regional profiles.

Calculation of the profiles for macro-regions based on regional profiles allows for a significant reduction in the cooper plate effect and

avoids unrealistically high estimation of RE technologies' FLh for macro-regions.

2.2. Applied scenario variations

The energy system transition is simulated considering the ambitious Best Policy Scenario (BPS) with a fast introduction of RE generation technologies in power generation and fast electrification of heat and transport sectors. The BPS definition is the same as used in Ref. [46] and Bogdanov et al. [47], who analysed this scenario in comparison with other less ambitious pathways. The BPS aims to reach the governmental target for 2030 and zero CO₂ emissions from the energy sector by 2050. At least 35 GW of solar photovoltaics (PV) must be installed in the years 2020–2025, and, by 2030, the share of RE in electricity generation must reach 40%, wherein the coal and nuclear power plants are assumed to be phased out by 2030. No additional nuclear reactors are restarted, and no new coal, oil, or nuclear power plants are commissioned. Coal use in industrial heat and processes is allowed until a full fossil ban in 2050. Commissioning of new gas-fired power plants is allowed; however, in later steps of the transition, these power plants switch to using sustainable e-methane and bio-methane.

In the transport and heat sectors, the BPS assumes rapid electrification: fast growth of electrical space and water heating shares in residential and commercial sectors, and fast reduction of internal combustion engine (ICE) vehicles shares in road transportation. By 2050, the share of battery-electric vehicles (BEV) in passenger transportation is assumed to exceed 76%, while the share of ICE and plug-in hybrid electric vehicles (PHEV) drops to about 13%. In freight transportation, the BEV share in 2050 is assumed to reach 67%, while ICE and PHEV still play a significant role with 26% of all freight transportation. Shares of hydrogen powered fuel cell electric vehicles (FCEV) are assumed to reach around 10% in passenger and 6% in freight road transportation. Rail transport is assumed to be fully electrified, whereas for marine and aviation transport, a conservative assumption of zero direct electrification is considered. To enable a gradual introduction of green fuels in the transport segments, the scenario sets minimum shares of green fuels consumption: at least 43% of liquid fuels in 2040 and 76% in 2045. Sustainable biofuels and locally produced and imported Fischer-Tropsch fuels are considered as such green fuels. Defossilisation of the energy system is supported by the growth of the carbon pricing from 2.4 €/tCO₂ in 2020 to 150 €/tCO₂ in 2050.

The financial and technical assumptions for the scenario, RE potential and energy demand assumptions for the scenario and respective references to the sources are presented in the supplementary material (Tables S1–S25) for each of the transition steps. The weighted average cost of capital (WACC) is set to 7% for all technologies.

This scenario is simulated using three different versions of the model.

Table 1
The solar PV and wind turbines full load hours.

Technology	Macro-region								
	Northeast			Centre		Southwest			
Standard RE profiles calculation routine for 9 sub-regions									
PV	1264	1256	1382	1232	1373	1334	1345	1342	1393
Onshore wind	3272	3094	2254	3004	2318	2998	3175	1561	3144
Offshore wind	4737	4413	4976	4343	4663	4323	3980	4340	4514
Standard RE profiles calculation routine for 3 macro-regions									
PV	1313			1357			1380		
Onshore wind	3030			2749			2930		
Offshore wind	4515			4325			4153		
Average of regional profiles with deviation to standard RE profiles									
PV	1300	(−1.0%)		1313	(−3.2%)		1360	(−1.4%)	
Onshore wind	2873	(−5.2%)		2773	(+0.9%)		2627	(−10.3%)	
Offshore wind	4709	(+4.3%)		4443	(+2.7%)		4278	(+3.0%)	

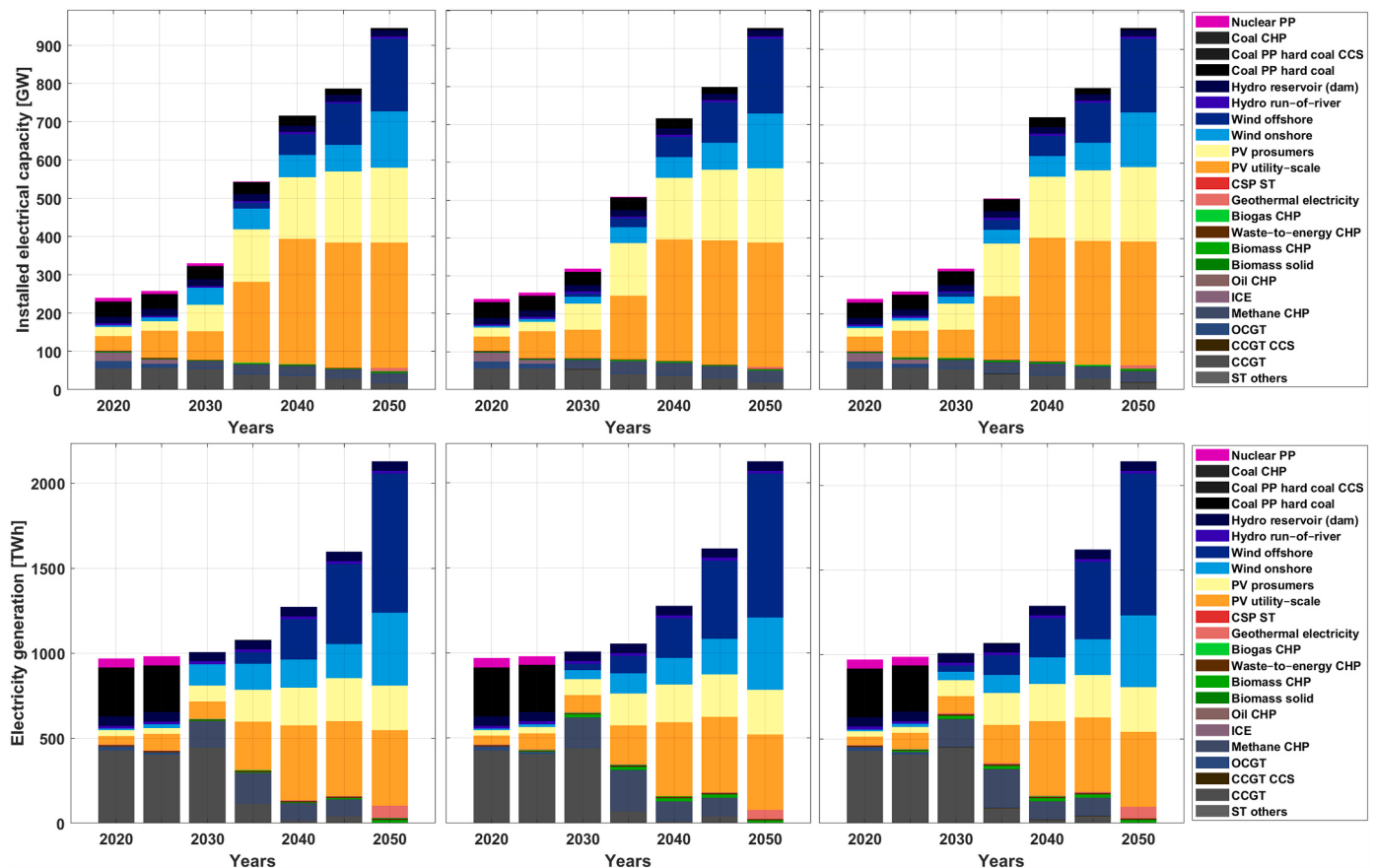


Fig. 3. Power capacity (top) and electricity generation (bottom) through the transition for the full 9 sub-regions simulation, 9Reg (left), hierarchical simulation with macro-regions RE profiles calculated as average of regional profiles, 3Mc_A (centre), and hierarchical approach with macro-regions RE profiles calculated based on profiles of individual nodes, 3Mc_St (right).

1. 9Reg: Standard approach with nine interconnected sub-regions simulation.
2. 3Mc_A: Hierarchical approach with macro-regions profiles calculated as an average of regional profiles
3. 3Mc_St: Hierarchical approach with macro-regions profiles calculated based on data in $0.45^\circ \times 0.45^\circ$ resolution applying the profiles integration per entire macro-region.

Outputs of the standard and hierarchical simulations have an identical format and are processed using the same scripts to calculate the system cost and other results.

3. Results

The application of the hierarchical approach to the Japanese energy

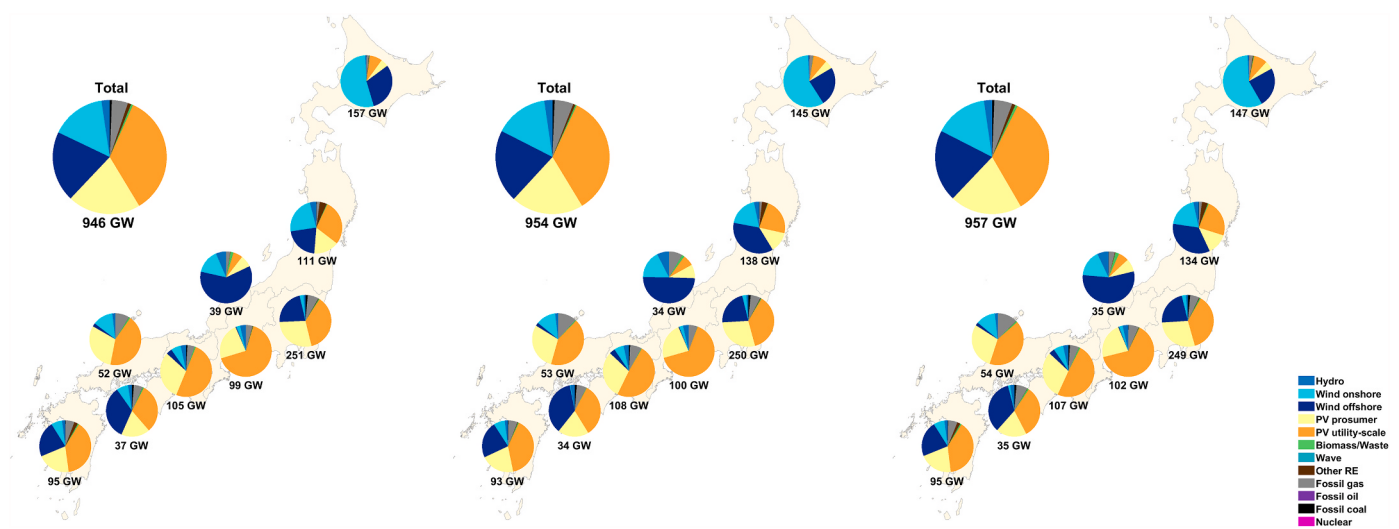


Fig. 4. Regional structure of power generation capacity in 2050 for the full nine sub-regions simulation (left), hierarchical simulation with macro-regions RE profiles calculated as average of regional profiles (centre), and hierarchical approach with macro-regions RE profiles calculated based on profiles of individual nodes (right).

system transition modelling does not result in a significant change in the results. The transition modelling in 9 regions resolution or applying the hierarchical approach results in a structural change of the energy system of Japan, from a mostly fossil fuels-based energy system to a 100% RE-based system in 2050. However, in all cases, the transition follows the same pathway; for each step of the transition, the energy system structure and costs are similar independently of the applied modelling approach.

Fig. 3 presents the structure of power capacity and generation through the transition for the standard approach (9Reg) and the comparison with the results using the hierarchical approach with macro-regions RE profiles calculated as an average of regional profiles (3Mc_A) and the hierarchical approach with macro-regions RE profiles calculated based on profiles of individual nodes (3Mc_St). The results for these three modelling designs are almost identical, in case of hierarchical simulations the total power generation capacity is 11 GW (1.2%) higher, mostly due to 1.2–1.6% higher wind capacity in the case of simulations based on a hierarchical approach. Correspondingly, wind generation is slightly higher in the case of the hierarchical simulation. Results in 3 macro-regions resolution (the second step of the hierarchical simulation) have shown higher deviations, the total power generation capacity is 20–32 GW (2.2–3.5%) higher compared to results of the standard modelling in 9 regions resolution, in particular due to wind power capacity that is 6.1–6.6% higher, as it is expected for the results in

lower special resolution. Higher deviations are seen for the case of capacity factors of macro-regions calculated as an average of the 3 sub-regions' capacity factors. The capacity and generation of the solar PV capacities do not change. Across scenarios, all available PV potential is utilised by the end of the transition as PV is the least cost source of electricity in 2050.

Though the role of wind generation increases in the case of the hierarchical approach, it affects the onshore and offshore wind generation differently: the capacity of offshore wind increases while the total capacity of onshore wind decreases. Likewise, the regional distribution of the generation capacities changes. In the case of the hierarchical approach simulation, the system tends to increase power generation capacities in northeastern sub-regions with high wind potential: Hokkaido and Tohoku, while reducing the capacity of the local onshore and offshore wind generation in southwestern sub-regions where wind turbines FLh are significantly lower. Fig. 4 presents the generation capacities structure in the sub-regions of Japan for the three scenarios.

At the second step of the hierarchical simulations, the system underestimates the cost of the electricity transmission inside the region. Annualised cost of the transmission grid in 2050 (including annualised capital costs and grid losses of the transmission grids between regions) on macro-regions step is 4–4.8 b€, while in full regional resolution the annualised cost of grids in 2050 is 11 b€. That has a significant impact for Japan due to the excellent wind generation potential in the distant

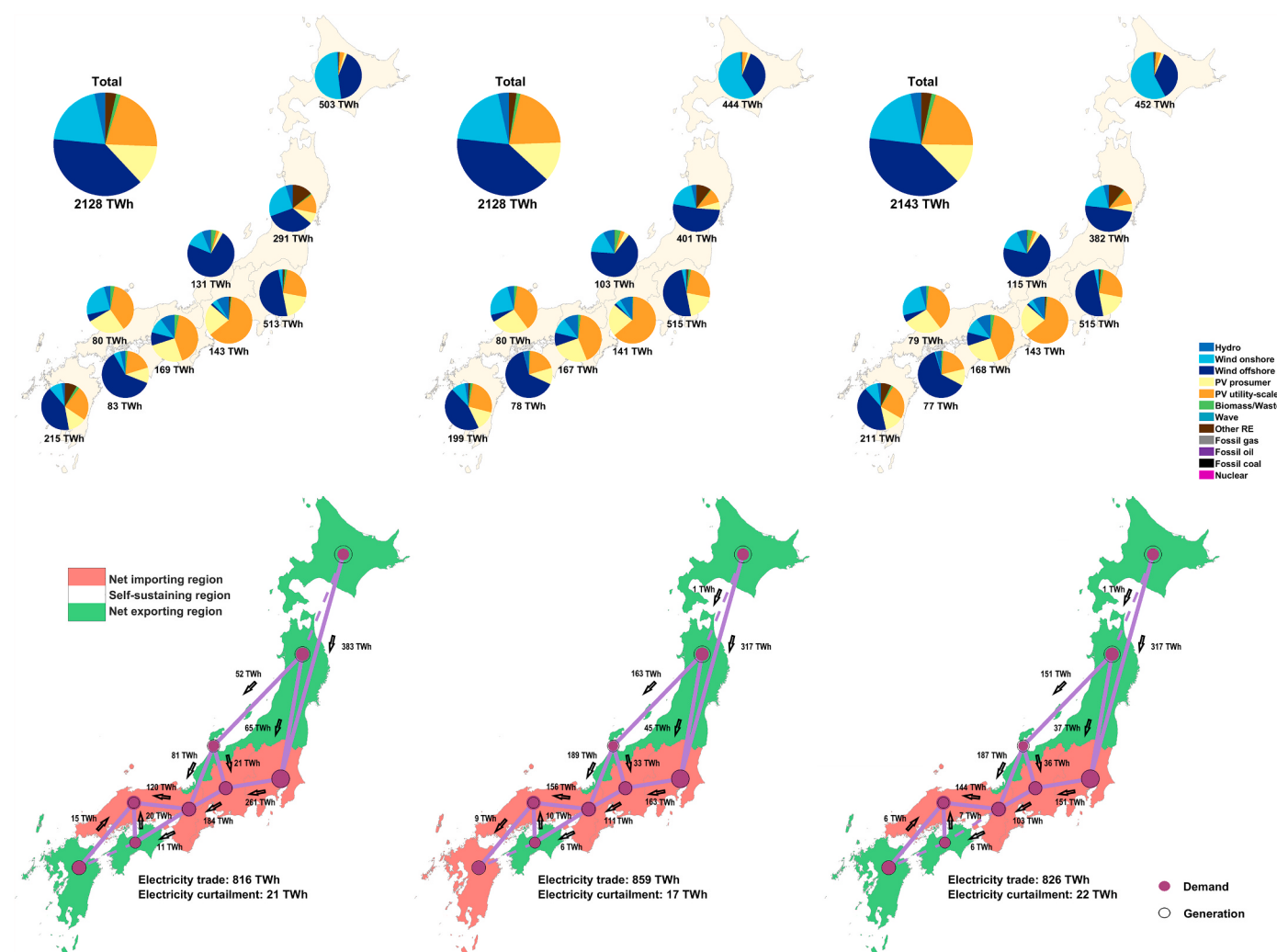


Fig. 5. Regional structure of power generation and power flows through the grids in 2050 for the full nine sub-regions simulation (left), hierarchical simulation with macro-regions RE profiles calculated as average of regional profiles (centre), and hierarchical approach with macro-regions RE profiles calculated based on profiles of individual nodes (right).

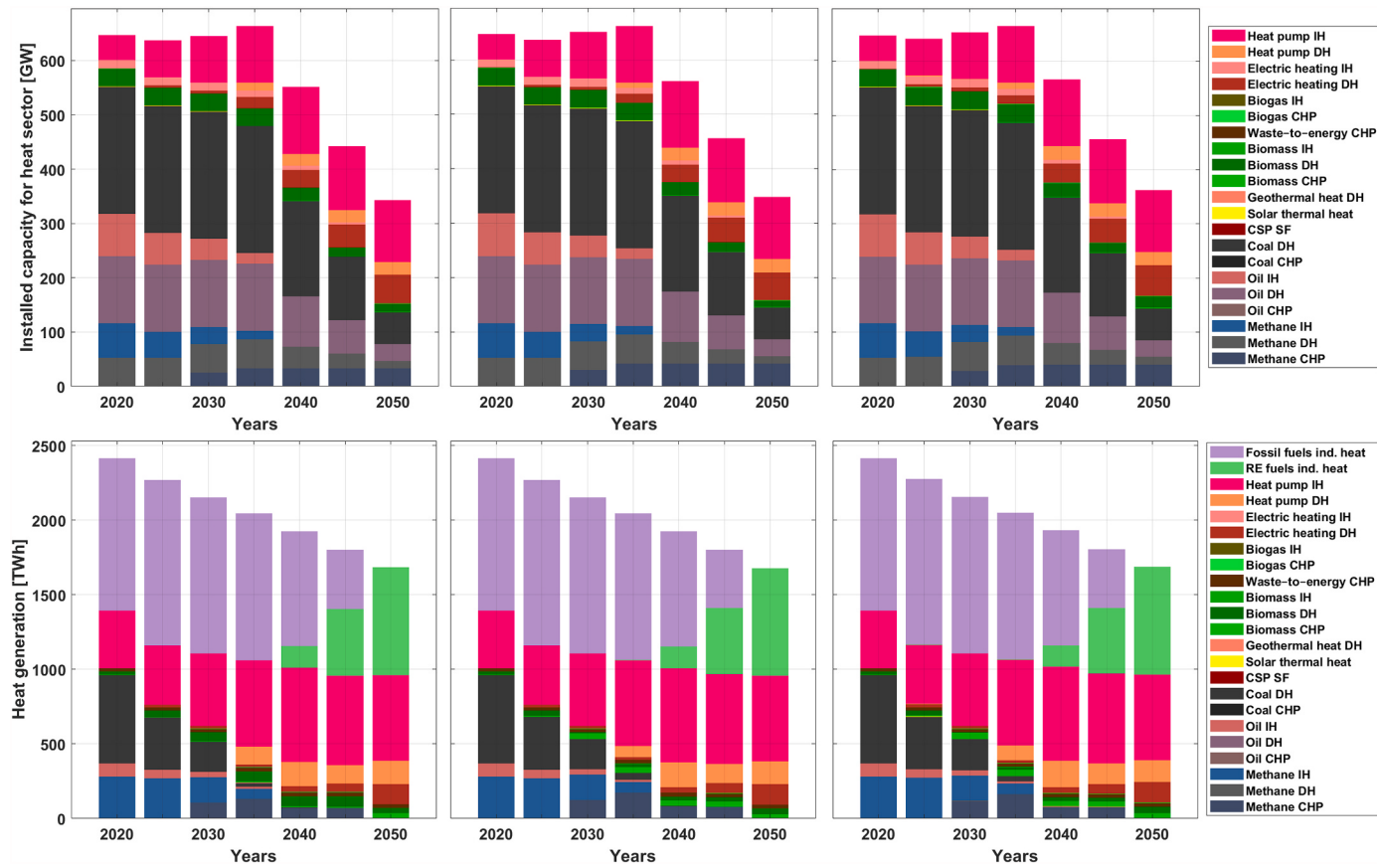


Fig. 6. Heat capacity (top) and generation (bottom) through the transition for the full 9 sub-regions simulation, 9Reg (left), hierarchical simulation with macro-regions RE profiles calculated as average of regional profiles, 3Mc_A (centre), and hierarchical approach with macro-regions RE profiles calculated based on profiles of individual nodes, 3Mc_St (right).

region of Hokkaido. Considering the low cost of electricity production and underestimated cost of the grid connection from Hokkaido to the Tokyo region and further to the south, hierarchical simulation results in higher electricity transmission from north to south than the full nine sub-regions simulation case, as induced in the second step of the simulation and thus as inherited power flows between macro-regions at the third step of the hierarchical simulation. In the final result of the hierarchical simulation, the annualised cost of grids in 2050 reaches 11.1–11.9 b€, slightly higher than for the full 9 sub-regions simulation. Fig. 5 shows the electricity generation and power flows through the grids in three simulation cases.

It is important to mention that most of grid investments occur in 2045–2050 when the local RE resources in Central and Southwestern regions are mostly exploited while the fossil energy supply is reduced to zero. While the system simulated with a hierarchical approach tends to

rely more on electricity imports from the northeast sub-regions of Hokkaido and Tohoku, the role of storage in electricity supply decreases. At the same time, electricity curtailment increases, especially in the northeast sub-regions. The electricity supply from northeast sub-regions does not simply cover the RE potential deficit in southern and central sub-regions, rather, it contributes to energy supply balancing to compensate for local RE supply variability. Additionally, the system tends to use more gas storage in the form of hydrogen and methane. The heat systems of all sub-regions are not interconnected; thus, a different simulation approach has no direct impact on the heating system, only indirect due to changes in the electricity generation profiles and LCOE in the sub-regions. Fig. 6 displays the heat capacity and generation structure by sources for the three simulation cases.

In the cases of the hierarchical approach the installed capacity is slightly higher at 2–18 GW, with biggest deviations in the 3Mc_St case,

Table 2

Energy carriers and system cost for the transition scenarios calculated by the three different modelling designs.

	Unit	Scenario	2020	2025	2030	2035	2040	2045	2050
LCOE	[€/MWh _{el}]	9Reg	106.9	110.5	119.4	108	88.1	77.9	68.2
		3Mc_A	106.9	110.6	122.3	112.3	89.7	78.9	68.4
		3Mc_St	106.9	112.1	123	112.8	90.4	79.6	69.4
LCOH	[€/MWh _{dh}]	9Reg	33.6	38.8	40.9	40.5	42.1	49.2	61.9
		3Mc_A	33.6	38.8	41.2	40.3	42.3	49.6	60.9
		3Mc_St	33.6	39.2	41.5	40.9	42.9	50.2	62.5
LCOEn	[€/MWh]	9Reg	51.3	56.8	63.3	61.9	59.7	62.1	64.8
		3Mc_A	51.3	56.8	64.1	63	60.5	62.8	65.3
		3Mc_St	51.3	57.6	64.5	63.7	61.4	63.7	66.3
Total ann. Cost	[b€]	9Reg	206	214	216	191	172	170	167
		3Mc_A	206	214	219	194	175	172	168
		3Mc_St	206	217	220	196	177	174	171

Table 3

Number of variables and optimisation time of the model for the three different modelling designs. The optimisation time comprises seven myopic steps each covering the 8760 h of a year modelled in perfect foresight.

	Variables		Constraints		Optimisation time [sec]		
	Macro	Regional	Macro	Regional	Macro	Regional	Total
9Reg		30,494,288		42,013,836			671,823
3Mc_A	10,082,998	10,118,040	13,823,567	13,911,156	59,232	145,336	204,568
3Mc_St	10,082,998	10,118,040	13,823,567	13,911,156	107,082	177,933	285,015

mostly due to gas and biomass-based district heating and CHP capacities, however, the share of these technologies in heat supply is minor, and these technologies are mostly used for peak shaving while the heat supply structure does not really change in the three cases, with total generation deviations within 1%. The results in the three macro-regions resolution (the second step of the hierarchical simulation) show a similar deviation on the level of 4–20 GW. Surprisingly the higher deviation is shown for the 3Mc_A case, the heat generation structure is similar to the one for the nine regions simulations with less than 2% difference in total generation. The transport sector energy demand is predefined by the scenario assumptions and does not change for the studied cases. While some deviations can be noticed, the overall system structure is still very similar, which consequently leads to similar system costs and cost of energy. Table 2 presents the results for the LCOE, levelised cost of heat (LCOH), levelised cost of energy (LCOEn), and total system cost.

While the impact of the different approaches can appear negligible for the long-term transition studies, the impact on the computation speed is much more significant. The hierarchical modelling approach shows robustness towards the systems' overall structure as the difference in individual technology capacity or energy costs remain within a ±3% range. At the same time, the hierarchical approach leads to a significant reduction of the model size in terms of the number of variables and, consequently, the time of the system optimisation. Table 3 shows the number of variables and optimisation time for the hierarchical and standard approach cases.

The optimisation time depends not only on the model structure, number of variables and constraints, and solver parameters, it is also dependent on the data inputs for the model. Despite the same model structure, solver parameters, and hardware used for both hierarchical simulation cases, the RE technologies capacity factors were different, leading to significant variations in optimisation times. Additionally, other processes could also compete for the computational resources of the user workstation and lead to considerable deviation in computational time. As a result, the computational time reduction for the hierarchical simulation case varies from 2.35 times in the case of the 3Mc_St scenario to 3.3 times in the case of the 3Mc_A scenario compared to the full computational time in full nine sub-regions simulation case.

4. Discussion

The results of the simulations show that the hierarchical approach for the simulation can lead to a significant reduction in computational time. The hierarchical approach with three macro-regions comprising three sub-regions each reduces the number variables and constraints on each of the simulation steps by a factor of 3 compared to the standard case where the nine sub-regions of Japan are simulated. The reduction of variables and constraints then leads to a reduction of the model size by a factor of 3 for each of the hierarchical simulation steps. That enables the simulation of more complex energy system models, with more comprehensive technological portfolios, more sectors considered and more sector coupling technologies, and higher temporal and spatial resolution.

The impact on the optimisation time is lower than the impact on the model size, the reduction of the total optimisation time is in the range of factors of 2.35–3.3, depending on the scenario, which represents a

substantial reduction. The time-series approach or spatial resolution reduction methods allow for more significant decreases in computational time. For the simulation with nine sub-regions regional structure, the reduction of computational time exceeds the additional time for data preparation for the macro-regions level, though exact time spent on data preparation cannot be defined by authors. The benefits increase, especially for research projects where multiple energy transition scenarios aiming for different policy targets are to be studied, initial assumptions are not perfectly defined and changing scenario definitions have to be considered, sensitivity analyses are carried out, etc. Another benefit is improved robustness to hardware and software failure. In the event of a potential workstation restart, the time loss is limited to the time consumed for a certain step of the hierarchical simulation, since the results of the previous step are already saved. Overall, the hierarchical approach has proven itself as an effective way to save time for energy system modelling.

The impact on the system structure can be noticed, but it is not significant. The variation of different technology shares in 2050 remains within ±1.5%, and the variation is higher in the 2030s. There, the 9Reg scenario leads to significantly faster defossilisation and higher reliance on onshore wind installations compared to the hierarchical simulation case. Later in the 2040s, the deviations in system structure reduce.

The main reason of deviations is the impact of lower spatial resolution on the RE potential estimation for the macro-regions step. At that step the deviation of the results is highest and then reduces at the third step of the hierarchical simulation, when each macro-region is modelled in higher spatial resolution. Still some deviations are inherited due to the use of power flows in grids adopted from the macro-regions level. One can see that the highest deviations are seen for the power sector, that relies on VRE electricity generation and is directly affected by power grid use, while the impact on the heat sector is smoothed as it consumes the electricity mix from the power sector. Overall, the hierarchical approach leads to a higher role of imported low-cost electricity and a lower role of local higher cost electricity, but for the case of Japan the impact is minor.

The impact on the system cost and the levelised cost of energy is not significant; in 2050, the costs are within ±2.5%, and even in the 2030s, the cost deviations do not exceed ±3%. The 3Mc_St results show the largest deviations compared to the nine sub-regions simulations, while the difference between the results of 3Mc_A and results of simulation for the nine sub-regions is much smaller and is within ±1% in 2050 and does not exceed ±2% through the transition.

These deviations are less than the deviations observed in case of applying the different time-series methods as shown by Kotzur et al. [35]. For some specific system configurations like CHP reliant or the residential system, authors found 'prediction errors less than 2%.' While the system cost stays roughly the same, one can see that the system structure in Kotzur et al. [35] changes significantly. Similarly, the regional resolution reduction also leads to significant deviations in the results [39]. The proposed hierarchical approach allows for the avoidance of these effects. Even though the deviations in the energy system structure after the first step of the hierarchical simulation are much higher, the second level simulation for individual macro-regions comprising the three sub-regions leads to improved results.

The range of deviations induced by the cost assumptions uncertainty can be much higher; as an extreme case, one can compare the fossil fuels

costs assumed by the International Energy Agency and other institutions for the period 2020 to 2025, and the fossil fuels prices in autumn 2021 to winter 2022. The capital costs are far less volatile, but the uncertainty of the technologies' capital and operational cost projections in 30 years' time horizon exceeds the uncertainty induced by the hierarchical simulations approach.

The hierarchical approach provides the possibility to significantly reduce the energy system simulation time without relevant changes to the simulation results. The core assumption of this method is that the power flows among macro-regions properly estimate the power flows among sub-regions in the full resolution case. In practice, though, the model tends to overestimate the grids utilisation as the cost of electricity transmission within the region remains unknown. That is the key reason for deviations between the scenarios, i.e. the higher share of onshore wind in the 2030s is the result of free access to the wind potential on Hokkaido island. Furthermore, an overall higher reliance on imports from northwestern sub-regions is a result of an underestimation of the grid costs from Hokkaido island, which makes these imports lower in cost than local production in central and southeastern sub-regions of Japan.

As power grid utilisation plays such an important role in hierarchical simulation, the proper definition of the macro-regions structure becomes very important. It should consider the existing grid structure, so that existing high-capacity lines connect the macro-regions; at the same time, sub-regions inside the macro-regions must share the borders, and the distance between these sub-regions' demand centres must be minimal in order to minimise underestimation of grid costs. Consequently, combining island sub-regions should be avoided as sea-connections are more expensive. Unfortunately, the macro-regions had to comprise several islands considering the overall structure of Japan; thus, the costs of exports from Hokkaido, as well as the cost of imports to Shikoku and Kyushu, were underestimated, which led to deviations in the hierarchical approach.

Although the import and export costs between regions were underestimated, the deviations between the simulation results were restricted by the limited RE potential of Japan. Considering the limited RE potential, the high energy demand, and PV CAPEX, the system had to utilise all available PV potential in all scenarios as PV was a lowest cost energy source with limited availability. Thus, the number of options for the system was limited and the remaining energy demand had to be covered with onshore or offshore wind power, either with local generation, or via imports from other sub-regions. In sub-regions with a higher PV capacity potential, the system would have more options to balance energy demand and supply, which could also lead to higher deviations in the results. Though in practice, this effect would be limited as the solar irradiation and therefore the PV yield potential is less site specific than the wind yield potential. For Japan, the PV yield difference between sub-regions of Japan is much lower than the one of wind power, thus higher PV potential assumptions could lead to even lower deviations in the results.

The wind power capacity potential is also almost fully used in all the regions, however, there one can see a substantial difference in results of the standard 9-regions simulation and the hierarchical simulations results: in the hierarchical cases the system tends not to use the local high cost wind generation in the Shikoku region, while in case of the standard 9-regions simulation the system reaches the upper limit of onshore wind power capacity in all regions.

Another limitation of the proposed algorithm is an arbitrary allocation of multiple grid connections between macro-regions, for example an additional power line between the Northeast macro-region and Central macro-region can be built to connect Tohoku to Hokuriku region, or Tokyo to Chubu. Currently the algorithm splits the capacity and power flows equally, but, as it can be seen in Fig. 5, in the standard 9-regions simulation case, the Tokyo to Chubu connection plays a far more important role.

The results of the simulation are also affected by the RE technologies

FLh profiles computation approach. The results show that for the case of this study, the method based on the calculation of an average for individual profiles of sub-regions included in the macro-region (3Mc_A) performed slightly better than the method based on the FLh profiles computation for the whole macro-region (3Mc_St). The results of the 3Mc_A scenario calculations were closer to the results of the standard nine sub-regions simulation; at the same time, the simulation time was about 40% higher compared to the 3Mc_St simulation. It is not clear how the outcome will change in the case of other regions' studies, but at least for the case of Japan, the FLh calculation approach is not a decisive parameter since the results of the system simulations were very close regardless of the chosen FLh calculations approach, and the hierarchical approach provides a significant gain in simulation speed.

For accurate macro-regions structure definition, the same approach can be applied to other regions of the world and on a global level. If a hierarchical approach was applied to a global simulation, the first level results on a major region level simulation (like Europe, Eurasia, Northeast Asia, etc.) will be naturally strongly affected by the copper plate effect. However, going further to macro-regions and sub-regions levels simulations will reduce the deviations introduced by the underestimation of energy transportation costs. Additional levels of simulation can be applied to improve the spatial resolution and further improve the accuracy of the results via reduction of the cooper plate effect. An example for a 4-level approach would be major regions in the world (level 1), macro-regions in Europe (level 2), Finland as a country in a Nordic macro-region (level 3) and Southeast Finland as a local region in Finland (level 4).

5. Conclusions

The results show that the hierarchical simulation approach can be applied to energy system transition studies. It results in a significant reduction of the model size and optimisation time, without a significant change in the simulation results compared to the simulation in full sub-regions resolution. The simulation on the chosen case of Japan structured the nine sub-regions via two steps of simulations, one for three macro-regions and the other for individual macro-regions comprising three sub-regions each. This led to reductions in computation time by factors of 2.35–3.3 compared to the standard simulation in nine sub-regions resolution. Such computational time reductions are driven by the decrease of model size on each step, which leads to a model that is 3 times smaller than standard simulation conditions. While the optimisation time decrease is significant, the structure of the resulting energy system and the cost of the energy stays within a ±2.5% range for the target year 2050. While the reductions in computation time should be on the same level for all regions whenever a similar macro-regions structure is applied, the impact of the hierarchical simulation approach on the results has to be further studied for other regions.

The hierarchical approach demands an accurate definition of the macro-regions structure on each hierarchical simulation step to minimise the impact of the grid costs and the FLh difference between sub-regions within the region in order to limit the cooper plate effect. The length of the grid connections within the macro-region should be at a minimum to minimise the impact of underestimated costs of the grid and losses in the grid. At the same time, sub-regions within the macro-region should have a comparable RE potential both in terms of installed capacity potential and FLh.

In energy transition studies, another question is how to calculate the macro-region's RE capacity factors profiles in order to further limit the copper plate effect. In the case of Japan, the two tested approaches of either averaging the more detailed sub-regions profiles or applying the profiles generation method to the entire macro-region as a whole demonstrate a similar performance. While one approach leads to closer simulation results, another allows for a more substantial reduction of the simulation time, but both are applicable in the case of Japan.

The hierarchical simulation approach can enable an increase in the

number of scenarios studied for each project given the same amount of time and computational resources. Otherwise, the approach can be used to facilitate studies with a higher temporal, spatial, or technological resolution, which could not be optimised with a standard full resolution approach considering computational limits. In the investigated case, the method was applied on two levels. First, one simulation on macro-regions level, and a second carrying out three parallel simulations for individual macro-regions comprising three sub-regions each, where each sub-region represents one of the nine mainland electric power companies' areas. In the case of Japan, a third level could be introduced to simulate in detail each of these electric power companies' areas in the prefecture's resolution.

More levels can be introduced, and this method can be applied to study global energy systems in high spatial resolution of 500–600 sub-regions or higher. There, each of these 500 to 600 sub-regions can be simulated not as energy islands, but with interregional energy flows a part of a global interconnected energy system.

Credit author statement

Dmitrii Bogdanov: Conceptualisation, Methodology, Investigation, Resources, Writing – Original Draft, Writing – Review & Editing, Visualisation.; **Ayobami Solomon Oyewo:** Resources, Writing – Review & Editing.; **Christian Breyer:** Conceptualisation, Methodology, Writing – Review & Editing, Supervision.

Declaration of competing interest

The authors declare that they have no known competing financial interests or personal relationships that could have appeared to influence the work reported in this paper.

Data availability

No data was used for the research described in the article.

Acknowledgements

The authors gratefully acknowledge the general support of LUT University. The authors would like to thank Gabriel Lopez for proofreading.

Appendix A. Supplementary data

Supplementary data to this article can be found online at <https://doi.org/10.1016/j.energy.2023.127213>.

References

- [1] [IPCC] - International Panel on Climate Change. Climate change 2022: mitigation of climate change. Contribution of working group III to the sixth assessment report of the intergovernmental panel on climate change. 2022. <https://doi.org/10.1017/9781009157926>. Cambridge, UK and New York, NY, USA.
- [2] [IPCC] - International Panel on Climate Change. Climate change 2014: mitigation of climate change. Cambridge and New York: Cambridge University Press; 2014. <https://doi.org/10.1017/CBO9781107415416>.
- [3] [IRENA] - International Renewable Energy Agency. Renewable power generation costs in 2021. 2022. Abu Dhabi.
- [4] Lazard. Lazard's levelised cost of energy analysis (version 15.0). 2021. New York.
- [5] Brown T, Schlachtberger D, Kies A, Schramm S, Greiner M. Synergies of sector coupling and transmission reinforcement in a cost-optimised, highly renewable European energy system. Energy 2018;160:720–39. <https://doi.org/10.1016/j.energy.2018.06.222>.
- [6] Connolly D, Lund H, Mathiesen BV. Smart Energy Europe: the technical and economic impact of one potential 100% renewable energy scenario for the European Union. Renew Sustain Energy Rev 2016;60:1634–53. <https://doi.org/10.1016/j.rser.2016.02.025>.
- [7] Breyer C, Khalili S, Bogdanov D, Ram M, Oyewo AS, Aghahosseini A, et al. On the history and future of 100% renewable energy systems research. IEEE Access 2022; 10:78176–218. <https://doi.org/10.1109/ACCESS.2022.3193402>.
- [8] Bogdanov D, Ram M, Aghahosseini A, Gulagi A, Oyewo AS, Child M, et al. Low-cost renewable electricity as the key driver of the global energy transition towards sustainability. Energy 2021;227:120467. <https://doi.org/10.1016/j.energy.2021.120467>.
- [9] Eyre N. From using heat to using work: reconceptualising the zero carbon energy transition. Energy Effic 2021;14. <https://doi.org/10.1007/s12053-021-09982-9>.
- [10] Prina MG, Manzolini G, Moser D, Nastasi B, Sparber W. Classification and challenges of bottom-up energy system models – a review. Renew Sustain Energy Rev 2020. <https://doi.org/10.1016/j.rser.2020.109917>.
- [11] Kittel M, Schill W-P. Renewable energy targets and unintended storage cycling: implications for energy modeling. iScience 2022;25. <https://doi.org/10.1016/j.isci.2022.104002>.
- [12] Brown T, Bischof-Niemtz T, Blok K, Breyer C, Lund H, Mathiesen BV. Response to 'Burden of proof: a comprehensive review of the feasibility of 100% renewable-electricity systems. Renew Sustain Energy Rev 2018;92:834–47. <https://doi.org/10.1016/j.rser.2018.04.113>.
- [13] Connolly D, Lund H, Mathiesen BV, Leahy M. A review of computer tools for analysing the integration of renewable energy into various energy systems. Appl Energy 2010;87:1059–82. <https://doi.org/10.1016/j.apenergy.2009.09.026>.
- [14] Heide D, Greiner M, von Bremen L, Hoffmann C. Reduced storage and balancing needs in fully renewable European power system with excess wind and solar power generation. Renew Energy 2011;36. <https://doi.org/10.1016/j.renene.2011.02.009>.
- [15] Rodríguez RA, Becker S, Andresen GB, Heide D, Greiner M. Transmission needs across a fully renewable European power system. Renew Energy 2014;63. <https://doi.org/10.1016/j.renene.2013.10.005>.
- [16] Breyer C, Bogdanov D, Aghahosseini A, Gulagi A, Fasihi M. On the techno-economic benefits of a global energy interconnection. Econ Energy Environ Policy 2020;9:83–102. <https://doi.org/10.5547/2160-5890.9.1.cbre>.
- [17] Galván A, Haas J, Moreno-Leiva S, Osorio-Aravena JC, Nowak W, Palma-Benke R, et al. Exporting sunshine: planning South America's electricity transition with green hydrogen. Appl Energy 2022;325:119569. <https://doi.org/10.1016/j.apenergy.2022.119569>.
- [18] Lopez G, Aghahosseini A, Child M, Khalili S, Fasihi M, Bogdanov D, et al. Impacts of model structure, framework, and flexibility on perspectives of 100% renewable energy transition decision-making. Renew Sustain Energy Rev 2022;164:112452. <https://doi.org/10.1016/j.rser.2022.112452>.
- [19] Østergaard PA. Reviewing EnergyPLAN simulations and performance indicator applications in EnergyPLAN simulations. Appl Energy 2015;154:921–33. <https://doi.org/10.1016/j.apenergy.2015.05.086>.
- [20] Lund H, Thellufsen JZ, Østergaard PA, Sorknaes P, Skov IR, Mathiesen BV. EnergyPLAN – advanced analysis of smart energy systems. Smart Energy 2021;1: 100007. <https://doi.org/10.1016/j.SEGY.2021.100007>.
- [21] Bogdanov D, Breyer C. North-East Asian Super Grid for 100% renewable energy supply: optimal mix of energy technologies for electricity, gas and heat supply options. Energy Convers Manag 2016;112:176–90. <https://doi.org/10.1016/j.enconman.2016.01.019>.
- [22] Bogdanov D, Farfan J, Sadovskaia K, Aghahosseini A, Child M, Gulagi A, et al. Radical transformation pathway towards sustainable electricity via evolutionary steps. Nat Commun 2019;10:1077. <https://doi.org/10.1038/s41467-019-08855-1>.
- [23] Bogdanov D, Gulagi A, Fasihi M, Breyer C. Full energy sector transition towards 100% renewable energy supply: integrating power, heat, transport and industry sectors including desalination. Appl Energy 2021;283:116273. <https://doi.org/10.1016/j.apenergy.2020.116273>.
- [24] HOMER Energy, HOMER; 2021. <https://www.homerenergy.com/index.html>.
- [25] Gils HC, Scholz Y, Pregger T, Luca de Tena D, Heide D. Integrated modelling of variable renewable energy-based power supply in Europe. Energy 2017;123. <https://doi.org/10.1016/j.energy.2017.01.115>.
- [26] Victoria M, Zhu K, Brown T, Andresen GB, Greiner M. Early decarbonisation of the European energy system pays off. Nat Commun 2020;11:6223. <https://doi.org/10.1038/s41467-020-20015-4>.
- [27] Jacobson MZ, Delucchi MA, Cameron MA, Mathiesen BV. Matching demand with supply at low cost in 139 countries among 20 world regions with 100% intermittent wind, water, and sunlight (WWS) for all purposes. Renew Energy 2018;123:236–48. <https://doi.org/10.1016/j.renene.2018.02.009>.
- [28] Elliston B, MacGill I, Diesendorf M. Comparing least cost scenarios for 100% renewable electricity with low emission fossil fuel scenarios in the Australian National Electricity Market. Renew Energy 2014;66. <https://doi.org/10.1016/j.renene.2013.12.010>.
- [29] Lenzen M, McBain B, Trainer T, Jütte S, Rey-Lescure O, Huang J. Simulating low-carbon electricity supply for Australia. Appl Energy 2016;179. <https://doi.org/10.1016/j.apenergy.2016.06.151>.
- [30] Duć N, Da Graça Carvalho M. Increasing renewable energy sources in island energy supply: case study Porto Santo. Renew Sustain Energy Rev 2004;8. <https://doi.org/10.1016/j.rser.2003.11.004>.
- [31] Pursiheimo E, Holttinen H, Koljonen T. Inter-sectoral effects of high renewable energy share in global energy system. Renew Energy 2019;136:1119–29. <https://doi.org/10.1016/j.renene.2018.09.082>.
- [32] Löffler K, Hainsch K, Burandt T, Oei P-Y, Kemfert C, von Hirschhausen C, et al. Designing a model for the global energy system—GENeSYS-MOD: an application of the open-source energy modeling system (OSeMOSYS). Energies 2017;10:1468. <https://doi.org/10.3390/en10101468>.
- [33] Victoria M, Zeyen E, Brown T. Speed of technological transformations required in Europe to achieve different climate goals. Joule 2022;6:1066–86. <https://doi.org/10.1016/j.joule.2022.04.016>.

- [34] IEA-ET SAP, TIMES; 2021. https://iea-etsap.org/index.php/etsap-tools/mod_el-generators/times.
- [35] Kotzur L, Markewitz P, Robinius M, Stolten D. Impact of different time series aggregation methods on optimal energy system design. *Renew Energy* 2018;117: 474–87. <https://doi.org/10.1016/j.renene.2017.10.017>.
- [36] Hoffmann M, Kotzur L, Stolten D. The Pareto-optimal temporal aggregation of energy system models. *Appl Energy* 2022;315:119029. <https://doi.org/10.1016/j.apenergy.2022.119029>.
- [37] Teichgraeber H, Brandt AR. Time-series aggregation for the optimization of energy systems: goals, challenges, approaches, and opportunities. *Renew Sustain Energy Rev* 2022;157. <https://doi.org/10.1016/j.rser.2021.111984>.
- [38] Frysztacki MM, Recht G, Brown T. A comparison of clustering methods for the spatial reduction of renewable electricity optimisation models of Europe. *Energy Informatics* 2022;5. <https://doi.org/10.1186/s42162-022-00187-7>.
- [39] Frysztacki MM, Hörsch J, Hagenmeyer V, Brown T. The strong effect of network resolution on electricity system models with high shares of wind and solar. *Appl Energy* 2021;291. <https://doi.org/10.1016/j.apenergy.2021.116726>.
- [40] Wang J, Kang L, Liu Y. A multi-objective approach to determine time series aggregation strategies for optimal design of multi-energy systems. *Energy* 2022; 258:124783. <https://doi.org/10.1016/j.energy.2022.124783>.
- [41] Mosek. MOSEK optimization toolbox for MATLAB 9.3.22. 2019. accessed March 18, 2021), <https://www.mosek.com/documentation/>.
- [42] Bogdanov D, Farfan J, Sadovskaya K, Fasihi M, Child M, Breyer C. Arising role of photovoltaic and wind energy in the power sector and beyond: changing the Northeast Asian power landscape. *Jpn J Appl Phys* 2018;57. <https://doi.org/10.7567/JJAP.57.08RJ01>.
- [43] Stackhouse P, Whitlock C. Surface meteorology and solar energy (SSE) release 6.0 methodology. Langley, VA, USA.: National Aeronautic and Space Administration (NASA); 2008.
- [44] Stackhouse P, Whitlock C. Surface meteorology and solar energy (SSE) release 6.0 methodology. Langley, VA, USA.: National Aeronautic and Space Administration (NASA); 2009.
- [45] Stetter D. Enhancement of the REMix energy system model: global renewable energy potentials, optimized power plant siting and scenario validation. Faculty of energy-, process- and bio-engineering, University of Stuttgart; 2012. PhD thesis.
- [46] Renewable Energy Institute, Agora Energiewende. Renewable pathways to climate-neutral Japan. LUT University; 2021.
- [47] Bogdanov D, Oyewo AS, Odai TNM, Nishida Y, Gagnébin M, Shimoyama T, et al. Energy transition for Japan: pathways towards 100% renewable energy system in 2050. 2023. submitted for publication.